Comparison of the Cytochrome bc_1 Complex with the Anticipated Structure of the Cytochrome b_6f Complex: De Plus Ça Change de Plus C'est la Meme Chose[1]

G. M. Soriano,[2,4] M. V. Ponamarev,[2] C. J. Carrell,[2] D. Xia,[3] J. L. Smith,[2] and W. A. Cramer[4]

Structural alignment of the integral cytochrome b_6-SU IV subunits with the solved structure of the mitochondrial bc_1 complex shows a pronounced asymmetry. There is a much higher homology on the *p*-side of the membrane, suggesting a similarity in the mechanisms of intramembrane and interfacial electron and proton transfer on the *p*-side, but not necessarily on the *n*-side. Structural differences between the bc_1 and b_6f complexes appear to be larger the farther the domain or subunit is removed from the membrane core, with extreme differences between cytochromes c_1 and *f*. A special role for the dimer may involve electron sharing between the two hemes b_p, which is indicated as a probable event by calculations of relative rate constants for intramonomer heme $b_p \rightarrow$ heme b_n, or intermonomer heme $b_p \rightarrow$ heme b_p electron transfer. The long-standing observation of flash-induced oxidation of only ~ 0.5 of the chemical content of cyt *f* may be partly a consequence of the statistical population of ISP bound to cyt *f* on the dimer. It is proposed that the *p*-side domain of cyt *f* is positioned with its long axis parallel to the membrane surface in order to: (i) allow its large and small domains to carry out the functions of cyt c_1 and suVIII, respectively, of the bc_1 complex, and (ii) provide maximum dielectric continuity with the membrane. (iii) This position would also allow the internal water chain ("proton wire") of cyt *f* to serve as the *p*-side exit port for an intramembrane H^+ transfer chain that would deprotonate the semiquinol located in the myxothiazol/MOA-stilbene pocket near heme b_p. A hypothesis is presented for the identity of the amino acid residues in this chain.

INTRODUCTION; SIMILARITIES

Between Cytochrome bc_1 And b_6f Complexes

The cytochrome bc_1 complex of the respiratory chain and the b_6f complex of oxygenic photosynthesis have long been known (Hauska *et al.*, 1983) to be similar in (a) their functions of (i) mediation of electron transfer between the major integral electron donor (dehydrogenases and photosystem II, respectively) and acceptor (cytochrome oxidase and photosystem I) complexes, (ii) electrogenic charge transfer and H^+ translocation; and (b) in the spectroscopically recognizable complement of redox prosthetic groups, which are present in the same stoichiometry, two b- and one c-type heme, one [2Fe-2S] cluster per unit complement

of polypeptides. (c) In addition, in both complexes, a bound lipophilic quinol/semiquinol is the electron and proton donor to the complex on the electrochemically positive side of the membrane and the complex. These properties have led to an emphasis in biochemistry/cell biology textbooks (Alberts *et al.*, 1994) on the common evolutionary background of the bc_1 and b_6f complexes. A molecular basis for this view was provided by comparison of the gene sequences and predicted distribution of hydrophobicity in integral membrane polypeptides of the complex, the mitochondrial and photosynthetic bacterial cytochrome *b* and the chloroplast cytochrome b_6-subunit IV (Widger *et al.*, 1984).

These many common properties of the core integral membrane proteins imply that membrane-embedded integral part of the complex diverges in evolution from a common origin. The *n*- and *p*-side extrinsic proteins of the bc_1 and b_6f complexes constitute a major difference between them. One might think that in early evolution, the only safe place for a protein to be in the presence of a scalding and highly charged external environment was inside a membrane. When things cooled down, the extrinsic proteins were attached to provide greater efficiency and, as discussed below, the mitochondrial and chloroplast precursors developed different solutions to the problem of a *p*-side high potential chain for oxidation of the *p*-side bound quinol (Q_p). A major theme of the present article is a discussion of mechanisms associated with the pathways of *p*-side plastoquinol oxidation based on the atomic or near-atomic structures of the mitochondrial cytochrome bc_1 complex (Xia *et al.*, 1997; Iwata *et al.*, 1998; Kim *et al.*, 1998; Zhang *et al.*, 1998). Details of the eleven subunit bc1 structure from bovine and avian mitochondria can also be found in the accompanying articles by Iwata *et al.*, Berry *et al.*, and Yu *et al.* in this volume. The properties of the seven subunits of the b_6f complex, the petA-D gene products involved in binding redox prosthetic groups, and the three small hydrophobic subunits, petG, petM, and petL that have been found to be present in *C. reinhardtii*, are summarized with polypeptide lengths and molecular weights corresponding to those in the *C. reinhardtii* complex (Table 1). Comparing the seven subunits with eleven of the mitochondrial cytochrome bc_1 complex, and 3-4 of the photosynthetic bacterial complex, it can be said initially that the four "large" subunits of the b_6f complex have structural and/or functional similarity. The three small (MW ca. 5,000) hydrophobic subunits are unique to the b_6f complex. All of the latter three may not be absolutely required, as a reading frame for petL is not found in the genome of the cyanobacterium Synechocystis sp. PCC 6803. The number of transmembrane helices in the intact complex would then be 11-12 per monomer [4 (cyt b); 3(SUIV); 1(cyt *f*); 1 (ISP); 2-3 (small hydrophobic polypeptides)]. The lipid content can be quite different, as there are 5 molecules per monomer of the unique lipid monogalactosyl-diacylglycerol present in the b_6f complex, along with one molecule each of chlorophyll a (Huang *et al.*, 1994) and β-carotene (Zhang *et al.*, 1999a). The one β-carotene must be positioned close to the Chl, as triplet state energy can be transferred from the latter to the former (Zhang *et al.*, 1999b).

Cytochrome *b*

The cytochrome *b* polypeptide in the bc_1 complex, consisting of approximately 380 and 440 residues in avian-bovine mitochondria and the photosynthetic bacteria *Rhodobacter sphaeroides* and *Rb. capsulatus*, respectively, is longer than the cyt b_6 polypeptide (214-215 residues in plant chloroplasts/green alga *Chlamydomonas reinhardtii*). The latter is equivalent in all known major structural and functional aspects to the N-terminal half of cyt *b* (bc_1) that binds the two *b*-hemes and contains the four trans-membrane helices A-D. The 160 residue suIV of the cyt b_6f complex appears to be a second cyt *b* gene product, and is analogous to the segment of cyt $b(bc_1)$ including the three trans-membrane helices, E-G, of cytochrome bc_1. Either cyt b_6-su IV are products of a gene that was "split" from the cyt *b* ancestor, or cyt(bc_1) is a fusion from the cyt b_6-su IV antecedent (Furbacher *et al.*, 1996). The prediction that the mitochondrial cyt *b* polypeptide would use the two histidine residues on the *n* and *p* sides of the B and D trans-membrane helices (Saraste, 1984; Widger *et al.*, 1984) was borne out in the solved atomic structure of the mitochondrial bc_1 complex (Xia *et al.*, 1997), and will almost surely turn out to be the same in cyt b_6 except for one additional residue between the histidine ligands on the 'D' helix (Widger *et al.*, 1984). The possible role of the extra residue between the two histidines on heme spectra and redox potentials (Cramer *et al.*, 1987; Kuras *et al.*, 1998), and the effect of the residue side chains that intervene between the hemes on interheme electron transfer will be considered below in the light of new structure data and concepts of long distance intra-protein electron transfer.

Table I. Properties of subunits of the cytochrome b_6f complex from *Chlamydomonas reinhardtii*

Subunit[a]	No. amino-acids	MW, (kDa)	No. TM helixes (predicted)	Reference
PetA (Cyt f) [c][b]	286	31.9	1	(Matsumoto *et al.*, 1991)
petB (Cyt b6) [c]	215	24.1	4	(Buschlen *et al.*, 1991)
petC (ISP) [n]	177	18.5	1	(de Vitry, 1994)
petD (SuIV) [c]	160	17.5	3	(Buschlen, 1993)
petG [c][c]	37	3.9	1	(Fong and Surzycki, 1992)
petL [c]	32	3.4	1	(Takahashi *et al.*, 1996)
petM [c]	39	4.0	1	(de Vitry *et al.*, 1996) & (Ketchner and Malkin, 1996)
		Total/monomer:	12	

[a] [c], [n] - chloroplast, nuclear - encoded
[b] small and large domains of elongated cyt f may correspond to the cytochrome c_1-subunit VIII subcomplex in cyt bc_1
[c] missing in cyanobacterium, *Synechocystis sp.* 6803

Asymmetric Transmembrane Distribution of Identical Residues Between Cytochrome b (bc_1) and b_6 (Similarity of Conserved p-Side Residues and Paucity of Conservation on n-Side)

Given the high degree of similarity in the hydropathy plots and heme coordination of cyt b(bc_1) and cyt b_6/suIV, the consequences of an alignment of the polypeptide chains of cyt b_6/suIV on the atomic structure of cyt b(bc_1) were investigated (Fig. 1). It is of interest that there is a significant degree of sequence-structure identity on the p-side of the complex (marked in red), and much less on the n-side. Besides the histidine ligands coordinating heme b_p, which was a basis for the alignment, a major region of identity is the Q_p quinone binding niche formed by the 'cd' and 'ef' extrinsic loops and the major loop on the p-side of helix E. Thus, it can be concluded that the mechanism of p-side quinol oxidation is likely to be very similar in the two complexes. It is also of interest, in the absence of a high affinity n-side quinone analogue inhibitor for the b_6f complex that the degree of n-side sequence-structure identity is small, mainly consisting of the residues that coordinate heme b_n. This raises the possibility that the nature of the putative Q_n quinone binding site differs significantly from that in the bc_1 complex and, along with the topological asymmetry in conserved residues implies that the mechanism for H^+ translocation in the b_6f complex on the n-side may differ in significant aspects from that in the bc_1 complex.

Identity of Residues in the Cluster-Binding Domain of the Rieske *ISP*

The high degree of similarity of the fold of the [2Fe-2S] cluster-binding domains of the ISP of the

bovine bc_1 and spinach b_6f complexes has been described (Carrell *et al.*, 1997). It is of interest in connection with the evolution of the complexes (see text, IA) that the fold of the ISP domain close to the quinol oxidation site and proximal to the membrane surface is far more conserved between bc_1 and b_6f complexes than the ISP domain that is distal relative to the membrane surface. The 139 residue p-side domain of the b_6f Rieske is also likely to have a mobile nature as judged by the presence of 6 Gly and 2 Pro in N-terminal 12 residues of the soluble p-side domain, the absence of defined electron density for these 12 residues in the atomic structure of the b_6f ISP (Carrell *et al.*, 1997) and a marked dependence of the rate of reduction of cyt f on lumenal viscosity (Heimann *et al.*, 1999). The mobility of the ISP is discussed below.

Dimer

Because the functional role of the dimeric complex is not known, it is also of interest that both complexes are dimeric, as shown from atomic structures of the mammalian mitochondrial bc_1 complex (Xia *et al.*, 1997; Iwata *et al.*, 1998; Kim *et al.*, 1998; Zhang *et al.*, 1998), and from analysis of the b_6f complex isolated from spinach chloroplasts (Huang *et al.*, 1994), the green alga, *C. reinhardtii* (Pierre *et al.*, 1995) and the cyanobacterium, *M. laminosus* (Huang *et al.*, 1999). However, see Chain and Malkin, (1991). A structurally obligatory nature of the dimer of the bc_1 complex seems implied by (i) the large area of monomer-monomer interaction, (ii) the inter-monomer crossover of the Rieske iron-sulfur protein, for which the trans-membrane helix is on one monomer and the extrinsic domain on the other, (iii) internal cavities in
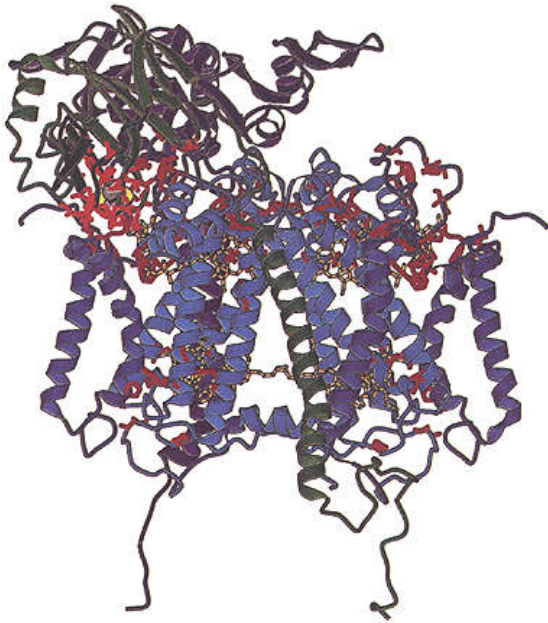
Fig. 1. Conservation of sequence and structure in the cytochrome b_6f/bc_1 family. Ribbon diagram is shown for the cytochrome b of the avian bc_1 complex (Zhang *et al.*, 1998), with the segments homologous to cytochrome b_6, and subunit IV, respectively, in light blue and dark blue. The Rieske protein is shown as a green ribbon. Heme b_p with an inhibitor in the Q_p site, and heme b_n with an inhibitor in the Q_n site are, respectively, at the top and bottom of the cytochrome b, drawn in orange. Invariant residues throughout the b_6f/bc_1 family are drawn in red for cytochrome b and in green for the Rieske protein. The invariant residues between cytochrome b and cytochrome b_6 are as follows, with numbering according to the avian cytochrome b: Helix A, n-side: P25, G35; helix A, p-side: G49; loop ab: Y56, A63, S66, G77; helix B, p-side: H84, A88, S89; helix B, n-side: H98, R101; helix C, n-side: W114, G117; helix C, p-side: G131, Y132; loop cd: L134, P135, Q138, W142, A153, P155, G158; helix D, p-side: T175, L176, R178, H183, P187; helix D, n-side: H197, P209. The invariant residues between cytochrome b and suIV are as follows, with numbering according to the chicken cyt b. Loop ef: P248, P262, T265, P266, I269, P271, E272, W273, Y274, I282, L283, K288; helix F, p-side: G291; helix F, n-side: P306. The known functions of these regions on the p-side are: (i) B and D helices, heme binding; (ii) cd, ef loops, loop on p-side of E helix, Q_p (stigmatellin niche); (iii) PEWY (Q_p near myxothiazol niche); (iv) other residues on surface helices of cyt b_6–suIV possibly used in interaction with ISP/cyt f. Invariant residues were obtained by alignment in CLUSTALW of the 22 known sequences of cyt b_6 and subunit IV with the N- and C-termini, respectively, of cyt b from 23 diverse sequences. The invariant residues between the bc_1 and b_6f Rieske ISP, with numbering according to the bovine ISP, are: G93, P95, C139, T140, H141, L142, G143, C144, C158, P159, C160, H161, G162, S163, Y165, G169, G174, P175, A176, P177, L180.

the complex that connect the Q_p niche on one monomer with the Q_n on the other (Xia *et al.*, 1997; Iwata *et al.*, 1998), and (iv) inter-monomer proximity between the two hemes b_p on the two monomers [Fe-Fe distance 5 21A; (Xia *et al.*, 1997)] that is the same as the Fe-Fe intra-monomer distance between heme b_p and b_n. The relative probability of heme $b_p \rightarrow b_p$ electron transfer is discussed below in the context of the possibility of " cross-talk" and interaction between the two monomers of the dimer.

DIFFERENCES BETWEEEN bc_1 AND b_6f COMPLEXES

The major differences between the bc_1 and b_6f complexes are listed below.

1. The 380-440 residue cyt $b(bc_1)$ polypeptide with eight TM helices A-H is replaced in the b_6f complex by two smaller integral polypeptides (cyt b_6 and subunit IV, ca. 215 and 160 residues, respectively) consisting of helices A-D and E-G (Fig. 1 and Widger *et al.*, 1984).

2. The large (MW 5 , 48 kD) n-side core processing polypeptides that are present in the mammalian mitochondrial bc_1 complex, but not in that from the photosynthetic bacteria, are also absent from the b_6f complex. There is no prominent protein mass extending from the n-side of the b_6f complex. One of the consequences may be difficulty in forming protein-protein contacts when the complex is crystallized in detergent.

3. A high affinity n-side quinone analogue inhibitor has not been found for the b_6f complex that is analogous to antimycin A in the bc_1 complex.

4. There is an extra threonine residue and a total of 14 instead of 13 amino acids between the two His ligands in the D helix (Widger *et al.*, 1984; Cramer *et al.*, 1987). It was proposed that the greater homogeneity of the b heme optical spectra and E_m's was a consequence of the extra residue in the D helix and/or the split cyt b gene product (Cramer *et al.*, 1987). The peaks of the a bands of heme b_n (561 nm) and heme b_p (split peak of 557.8 and 565.7 nm) in wild type bacterial *Rb. sphaeroides* cyt b are clearly distinct. However, in cyt b_6, the a band peaks of the two hemes have virtually indistinguishable peaks, 563-564 nm in almost all studies, in reduced minus oxidized spectra. The structural origin of these differences between cyt b_6 and cyt $b(bc_1)$ was tested by mutagenizing cyt $b(bc_1)$ of *Rb. sphaeroides* into a "b_6-like" polypeptide by (a)

inserting a threonine in position 199 (199T mutant) or (b) constructing a "split" cyt b_6 in the cyt bc_1 complex of *Rb. sphaeroides* (Kuras *et al.*, 1998). Each of these two site-directed mutants did, in fact, result in a significant degree of homogenization of either the cyt b spectra or the redox parameters, but not both, to values more characteristic of the b_6f complex. Thus, the "b-split" mutant caused red and blue shifts of hemes b_n and b_p, respectively, resulting in a decrease of the $\Delta\lambda_{max}$ from 4-5 to 2 nm. The T199 insertion mutant resulted in an increase in the E_m of heme b_p and consequently in a decrease of the ΔE_m from 140 to 50 mV. It would be interesting, therefore, to characterize a double ("b-split" + "insertion") mutant.

5. Cytochromes f and c_1 are completely different proteins. These two cytochromes are completely different in terms of both sequence and structure, except for both being c-type cytochromes with the characteristic Cys-X-Y-Cys-His c-heme binding sequence motif. Considering the p-side extrinsic domains, the unique features of the 252 residue domain of cyt f are (i) its β sheet secondary structure; (ii) a domain structure, with the large and small domains consisting, respectively, of residues 1-168 and 232-247, and 169-231; (iii) the alpha-amino group of the N-terminal residue as the sixth (distal orthogonal) ligand in 23 cyt f sequences the N-terminus is always occupied by an aromatic residue (Tyr in 20 of 23). This aromat and one at position 4 provide shielding for the heme from the aqueous phase and thus make a large contribution to the very positive E_m of cyt f (+0.37 V vs. 0.22 V for cyt c_1). Cytochrome f also contains (iv) a buried internal chain of five water molecules. This water chain is a conserved feature of the structure, with occupancy in the structure and temperature factors the same as in the adjacent atoms of the polypeptide chain. All side chain and back-bone residues that contribute H-bonds to the chain are virtually conserved in the 23 cyt f sequences. The H_2O chain is also present not only in cyt f from higher plants (Martinez *et al.*, 1996), but also in that from the green alga *C. reinhardtii* (Berry *et al.*, 1997) and the primitive thermophilic cyanobacterium, *P. laminosum* (Carrell *et al.*, 1999). The internal water chain, which contains an 11 Å linear segment of four waters, is unique among known protein structures. Its structure suggests that it may serve as a "proton wire" in an exit port for H^+ translocated across the membrane by the cyt b_6-suIV integral part of the complex. No such water chain has yet been seen in the structure of cyt c_1, which could be a consequence of the level of resolution in the x-ray crystallographic analysis of the bc_1 complex.

It was previously suggested, based on the resemblance of the folding motif of cyt f to plasma membrane receptor proteins, that cyt f protruded significantly from the membrane in order to more efficiently interact with its electron acceptor, plastocyanin (Martinez *et al.*, 1994). Based on EPR studies of cyt f in oriented membranes [discussed in (Martinez *et al.*, 1994)], it was proposed that the long axis of cyt f subtended an angle of $25°-30° \pm 10°$ with the plane of the membrane with a broad half-width in the angular distribution. The projection of cyt f on the membrane surface would then be approximately 64 Å which is similar to the length of the electron density attributed to cyt f in an 8 Å EM projection map of negatively stained b_6f complex from *C. reinhardtii* (Mosser *et al.*, 1997). In spite of this approximate correspondence, it is now hypothesized that the p-side domain of cyt f lies parallel to the membrane surface, presumably interacting with the surface helices of cyt b_6-suIV, with the average orientation of the heme constrained to satisfy the EPR data. The large and small domains of cyt f would then be structurally approximately analogous to the extrinsic domains of the cyt c_1 and suVIII (Figs. 2A, B). The purpose of the elongated structure of cyt f and its small domain would be to act as p-side surface "dielectric molding" for the core subunits of the complex to provide structure stability. The main reasons for proposing a surface-bound location for cyt f are (i) to allow its H_2O chain to accept H^+ from the oxidation site of the semiquinone near heme b_p, inferred from the binding of myxothiazol/MOA-stilbene in the bc_1 complex. It is assumed that mobility of the ISP in the p-side aqueous phase precludes H^+ transfer to cyt f. (ii) The inference, based on the consequences of mutagenesis of cyt f residues that provide H-bonds to the buried H_2O, that electron transfer from ISP to cyt f requires co-transfer of H^+ (Ponamarev and Cramer, 1998). Electrostatic constraints on e^-/H^+ transfer are most readily understood if cyt f is contiguous with the membrane and the low dielectric medium is continuous from the membrane interfacial region into cyt f. In the context of motional properties of the ISP [(Zhang *et al.*, 1998); Iwata *et al.*, this volume], it is of interest that the broad angular distribution of the cyt f heme relative to the plane of the membrane suggests the possibility of a narrow range of possible orientations about the long axis of cyt f. It is possible that such motional possibilities would facilitate the docking of plastocyanin and the ISP. It should be noted that the
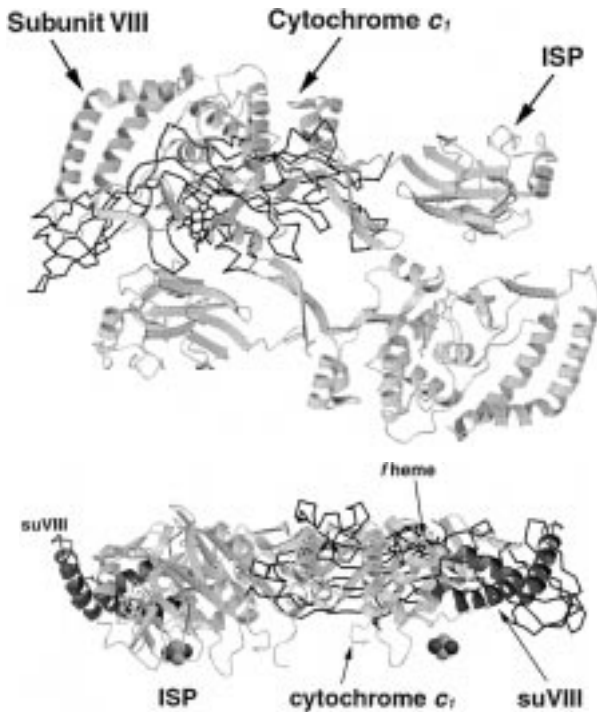
Fig. 2. Model of 252 residue *p*-side soluble fragment of 285 residue cyt *f* from turnip chloroplasts (Martinez *et al.*, 1996) [bold] superimposed on *p*-side domain of cyt c_1 and subunit VIII of the avian mitochondrial bc_1 complex (Zhang *et al.*, 1998). (A) Top view of *p*-side of dimeric bc_1 complex. The cyt c_1, ISP, and suVIII subunits of the bc_1 complex have been rendered as ribbons, and cyt *f* is drawn in bold in a wire format. Cytochrome *f* has been laid lengthwise along the dimer of cyt bc_1. Both sets of subunits of the whole dimer are included, while only one cyt *f* molecule is shown. (B) Side view of part of *p*-side of bc_1 complex. Only cyt c_1, suVIII, and the [2Fe–2S] cluster are shown. Figures drawn using MOLSCRIPT and RASTER3D (Kraulis, 1991; Merritt and Murphy, 1994).

docking requirements of the former for electron transfer are not necessarily very stringent. No specific surface region of cyt *f* has been shown to be required for oxidation of cyt *f* by plastocyanin in vivo (Soriano *et al.*, 1996; 1998).

INTERACTION BETWEEN CYTOCHROME *f* AND THE RIESKE ISP

Four-Step Reduction of Cytochrome *f*

The polyGly/polyPro linker to the membrane domain of the soluble domain of the b_6f ISP suggests that it is at least as mobile as it is in the bc_1 complex where it can undergo a reversible tethered translation

of 10–15 Å and a rotation of 55–60° about an axis passing near residues 93 and 182 (Zhang *et al.*, 1998). The tethered diffusion of the ISP implies that the electron transfer between the quinol at the Q_{p1} (stigmatellin) site and cyt c_1 or cyt *f* should be considered as at least, a four step process: (i) quinol deprotonation (ii) electron transfer from the anionic quinol to the ISP at the Q_{p1} interface; (iii) diffusion of ISP from the Q_{p1} site to a docking site on or near cyt *f*, possibly via a discrete intermediate position seen in the bc_1 atomic structure of (Iwata *et al.*, 1998), (iv) electron transfer from the ISP to cyt *f*.

Classical Low-Amplitude Reduction of Cytochrome *f* by ISP; Statistical Distribution of ISP-cyt *f* Complexes in the Dimer.

A rate constant of 10^4–10^5 sec^{-1} for the electron transfer from ISP to cyt *f* in step (iv) (Whitmarsh *et al.*, 1982; Crofts and Wang, 1989) would account for cyt *f* oxidation by single saturating flashes having an amplitude 0.5 that of the chemical content of cyt *f* in the membrane. These data could be reconciled by the role of a slow step in the multistep reduction of cyt *f* associated with quinol deprotonation and/or the tethered diffusion, and a statistical distribution of ISP binding sites in the dimer, ISP-*f*, ISP-Q_{p1} and perhaps ISP in an intermediate position. In the initial dark state before imposition of the light flash, it is proposed that ~0.5 ISP is bound to cyt *f* ("*f* site"), perhaps, in only one of the monomers. The remainder of the ISP is either in the intermediate state described by (Iwata *et al.*, 1998) or bound near the Q_{p1} site. The oxidation of the sub-population of cyt *f* to which the ISP is bound would not be observed because of the large rate constant for ISP → cyt*f* electron transfer. The reduction of the remaining cyt *f* in the other monomer would occur at the rate limiting step for its reduction at the Q_{p1} site and subsequent diffusion to cyt *f*.

With respect to the high (10^4–10^5 sec^{-1}) rate constant for ISP → cyt *f* electron transfer rate (Crofts and Wang, 1989), the decrease of a factor of 3 and 13 in the rate of cyt *f* reduction in N-terminal Y1S and P2V mutants (Zhou *et al.,* 1996) relative to wild type could be explained by Marcus theory (Marcus and Sutin, 1985) taking into account a decreased E_m of the mutants and assuming that $k_{et} \approx 200$ s^{-1} ($t_{1/2} \approx 3$ ms) [Table 2; Ponamarev, 1999]. This suggests that the rate constant for the reduction of cyt *f* by the ISP could be much smaller than 10^4–10^5 sec^{-1}.

Table II. Comparison of Measured and Calculated ISP $\rightarrow$ Cytochrome f Electron Transfer Rates: Mutants Y1S and P2V of Cytochrome f vs. Wild Type

Strain	$_{1/2}$, (ms)^a reduction	ΔE_m(mV)	ΔG^o(eV)	$\exp(\Delta G^\ddagger/RT)$ $\times 10^4$	F_c	F_{exp}
WT	3	75	−0.075	2.491	—	—
Y1S	9	18	−0.018	0.836	3.0	3.0
P2V	40	−55	0.055	0.198	12.6	13.3

^{a} half-times for the ISP-mediated reduction of cyt f *in vivo* in wild type and mutants (Zhou *et al.*, 1996); F_c - calculated inhibition factor for cyt f reduction kinetics; F_{exp} - inhibition factor obtained from experiment; Equations used in calculations: activation energy for electron transfer, $\Delta G^\ddagger = (\lambda + \Delta G^o)^2/4\lambda$; $\Delta G^o = -nF\Delta E_m$; $\Delta E_m = E_m(\text{cyt } f) - E_m(\text{ISP})$. Reorganization energy, $\lambda = 1$ eV (typical value for ET in protein systems (Moser *et al.*, 1995; Gray and Winkler, 1996); $E_m(\text{ISP}) = 295$ mV.

Coupling of Electron and Proton Transfer in Cytochrome f

The inhibited rates of cyt f reduction in site-directed mutants of residues that provide H-bonds to the internal H_2O chain of cyt f imply a critical role of the H_2O chain in function, and specifically in coupled electron and H^+ transfer. The mutants showed a large (2–6 fold) decrease in the rate of cyt f reduction, but no effect on the rate of reduction of cyt b_6 (Ponamarev and Cramer, 1998), so that the reduction of high and low potential chains appears "non-concerted." The decrease in rate of cyt f reduction did not correlate with the decrease in midpoint potentials in the mutants. The non-concerted transfer could be explained if plastocyanin can bypass the ISP, as implied by the positions of cyt $c1$ and the ISP in the bc_1 complex, and if there is no specificity in the binding site requirement for PC *in vivo* as inferred from PC-cyt f interaction (Soriano *et al.*, 1996; 1998). Then, a direct ISP-PC interaction competent for electron transfer does not seem to be precluded. The physiological need for a "cyt f bypass" pathway is not known. Evidence for such a pathway involving the small amplitude of cyt f turnover compared to P700 has been discussed previously (Haehnel, 1975). The faster reduction of cyt b_6 compared to cyt f, which is observed in normal chloroplasts (Selak and Whitmarsh, 1982), and in media of increased viscosity (Heimann *et al.*, 1999), also implies a "cyt f bypass".

## ELECTRON AND PROTON TRANSFER ON THE *p*-SIDE OF THE MITOCHONDRIAL CYTOCHROME bc_1 COMPLEX.

Pathways of Electron Transfer

Given recent developments in the theory of long distance intraprotein electron transfer (Farid *et al.*, 1993; Beratan and Onuchic, 1996; Gray and Winkler, 1996), new information on the atomic structure of the mitochondrial cyt bc_1 complex, and the possibility of differences in detailed mechanism between b_6f and bc_1 complexes, the following questions can be addressed about pathways of electron transfer in the mitochondrial bc_1 complex.

Pathway of $b_p \rightarrow b_n$ Interheme Electron Transfer

Does the pathway of $b_p \rightarrow b_n$ electron transfer utilize the connecting "B" and "D" helices (Fig. 3A), or does it pass through the space intervening between the hemes, (a) either directly or (b) via a one-stop pathway that utilizes the side chains that protrude between the hemes (Fig. 3B). The favored ET pathway depends on the interheme distance, the role of the protein in electron transfer, and the activation energy, $\Delta G^\ddagger$, which is a function of the ΔE_m and the reorganiza-
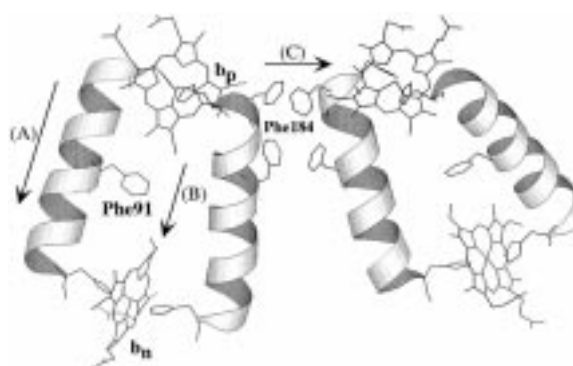
Fig. 3. Pathways of intra- and intermonomer heme–heme electron transfer. Heme $b_p \rightarrow b_n$ intramonomer electron transfer via (A) the connecting helixes and (B) through-space. (C) Most likely pathway of intermonomer $b_p \rightarrow b_p$ electron transfer. Figure was drawn using MOLSCRIPT (Kraulis, 1991).

tion energy, λ, associated with the electron transfer. Relative rates of electron transfer through different pathways can be calculated by considering (a) the algorithms for attenuation of electron transfer through the different structure elements and (b) the activation energy for the transfer. Using a formalism in which the distance dependence of the ET rate constant, k_{et}, is resolved into different dependences for covalent-bond, H-bond, and through-space transfer (Beratan and Onuchic, 1996): (i) covalent bond, $\varepsilon_C = 0.6$; (ii) H-bond, $\varepsilon_H = 0.36 \exp[-1.7(R-2.8)]$; (iii) through-space, $\varepsilon_S = 0.3 \exp[-1.7(R-1.4)]$. The donor-acceptor attenuation factor, TDA, after electron transfer through "i" covalent, "j" hydrogen bonds, and "k" through-space jumps is $\prod_i \varepsilon_C \prod_j \varepsilon_H \prod_k \varepsilon_S$ and k_{et} is proportional to $(\text{TDA})^2$.

Through-Helix vs. Through-Space Pathway For Heme $b_p \rightarrow b_n$ Inter-Heme Electron Transfer

For transfer from heme b_p to heme b_n, through two His heme ligands (5 covalent bonds to the heme Fe for each histidine in helix B or D) and the 13 or 14 residues in the "B" or "D" trans-membrane helices between these His residues, through a pathway down the helix that includes 15 covalent and 3 H-bonds, $(\text{TDA})^2 = 2.3 \times 10^{-15}$ (Table 3). For through-space transfer across the 7.6 A that separates the nearest side-chains of the hemes (in pdbbgy.ent, protein databank), $(\text{TDA})^2 = 2.4 \times 10^{-15}$. Thus, the probabilities for $b_p \rightarrow b_n$ electron transfer through two pathways are essentially identical. The existence of two helix connections between the hemes may further enhance the use of the through-helix pathway. These attenuation factors are activation-less. The transfer rate will be further diminished by a factor of 6×10^{-3} due to the Franck-Condon (activation energy) term, $\Delta G^{\ddagger} = (\Delta G^o + \lambda)^2/4\lambda kT$, where λ is the reorganization energy, 0.7 eV for intra-membrane electron transfer (Farid *et al.*, 1993) $\Delta G^0 = -0.1$ eV for ET from heme b_p to heme b_n, and RT = 0.025 eV at room temperature. The activation energy is assumed to be the same for both of the pathways connecting hemes b_n and b_p, and the relative rates of electron transfer through them are not affected by including it in the calculation. We note that a major factor in the attenuation of the through-space relative to the through-helix pathway is the assumption that the metal-metal distance is more appropriate for transfer between two transition-metal complexes (Gray and Winkler, 1996). If the appro-

priate distance is edge-edge, the two pathways again have comparable probabilities, but the probability of the through-space pathway is slightly greater. We note that the absolute value of the predicted ET rate constant is closer to the measured value if edge-edge distances between the hemes are used in the calculation.

Through-Space Transfer; Effect of Intervening Side Chain

An additional structural feature that might affect $b_p \rightarrow b_n$ transfer is the prominent intervening side chain in the "through-space" region between b_p and b_n, is the aromat, Phe91, which might facilitate inter-heme ET (Cramer *et al.*, 1987). It was noted in the latter work that such an aromatic residue was present in the bc_1 but not in the b_6f complex, where it was replaced in the spinach cyt b_6 by methionine. Using through-space distances of 3.9 and 4.3 A, respectively, from the Fe of heme b_p to Phe91, and from Phe91 to the Fe of heme b_n, $(\text{TDA})^2 = 3.3 \times 10^{-15}$. This calculation is obviously very sensitive to the values of the heme-Phe distances. The values of these distances in the structure (E. Berry, pers comm.) are 5.1 and 4.43 A, leading to a value of $(\text{TDA})^2 = 3.7 \times 10^{-17}$. The larger of the $(\text{TDA})^2$ values, for residue-mediated through-space transfer is comparable to the value of 2.4×10^{-15} for through-space transfer without an intervening step. Thus, the probability of through-space inter-heme $b_p \rightarrow b_n$ pathway seems not to be affected very much by an intervening residue and both values are at best comparable to through-helix pathways. This would explain why the nature of the intervening residue was found to have no effect on the electron transfer rate (Yun *et al.*, 1992).

Inter-Monomer Electron Transfer Between the Two Hemes b_p

The observations (a) that the distance between the Fe atoms of the two hemes bp, ca. 21 A, is approximately the same as that between those of heme b_p and b_n (Xia *et al.*, 1997) and (b) of the presence of aromatic residues (e.g., Phe184) in the dimer interface that might facilitate inter-monomer heme $b_p \rightarrow b_p$ electron transfer, raise the question of electron sharing between the two hemes b_p of the dimer, and of the function of the dimer. $(\text{TDA})^2$ for the inter-monomer heme b_p-heme b_p electron transfer ranges from 2.4×10^{-13} to 2.8×10^{-12}, assuming 10 covalent bonds between Phe184

Table III. Calculated attenuation, $(T_{DA})^2$, and Franck–Condon Factors for Intra-Monomer Heme $b_p \to b_n$ and Inter-Monomer heme $b_p \to b_p$ Electron Transfer

Pathway	Mode of transfer	$(T_{DA})^2$	Franck–Condon Factor (F.C.)	$(T_{DA})^2 \times$ F.C.
I. $b_p \to b_n$				
1. α helix	15 covalent bonds 3 H bonds 5 covalent bonds from His to Fe ($\times 2$) = 10; total of 25 covalent bonds	2.3×10^{-15}	5.8×10^{-3}	1.3×10^{-17} (1.0)
2. Through-space	7.6 A (Iwata) 5 covalent bonds from methyl group to Fe/heme ($\times 2$) = 10 covalent bonds	2.4×10^{-15}	5.8×10^{-3}	1.4×10^{-17} (1.1)
3. Through-space, through Phe91	3.9 A, 4.3A (Iwata *et al.*, 1998) 5 covalent bonds from methyl group to Fe/heme ($\times 2$) = 10 covalent bonds	3.2×10^{-15}	5.8×10^{-3}	1.9×10^{-17} (1.5)
	5.1 A, 4.4 A (E Berry, pers. comm); 5 covalent bonds from methyl group to Fe/heme ($\times 2$) = 10 covalent bonds	3.7×10^{-17}	5.8×10^{-3}	2.1×10^{-17} (1.6)
II. $b_p \to b_p$	10 covalent bonds from Fe to Phe 184 per monomer ($\times 2$) = 20 covalent bonds			
	2.5 A (Kim *et al.*, 1998)	2.8×10^{-12}	9.1×10^{-4}	2.5×10^{-15} (192)
	3.0 A (Iwata *et al.*, 1998)	5.8×10^{-13}	9.1×10^{-4}	5.3×10^{-16} (41)
	3.2 A (E Berry, pers. comm.)	2.4×10^{-13}	9.1×10^{-4}	2.2×10^{-16} (17)

^{a} $T_{DA} = \prod_i \varepsilon_C \prod_j \varepsilon_H \prod_k \varepsilon_S$. Franck–Condon factor $= \exp(-\Delta G^o + \lambda)^2/4\lambda kT$, $\lambda = 0.7$ ev; $\Delta G^0 = -0.1$ and 0 ev for $b_p \to b_n$ and intermonomer $b_p \to b_p$ electron transfer. Numbers in parentheses are normalized total attenuation factors.

and heme b_p in each monomer, and a through-space distance between the two Phe184 (adjacent to His183, which is one of the D-helix ligands of heme b_p) at the inter-monomer interface that ranges from 2.5–3.3 A in the structures of (Xia *et al.*, 1997; Iwata *et al.*, 1998; Zhang *et al.*, 1998). This also takes into account the increase in $\Delta G^{\ddagger}$ for $b_p \to b_p$ electron transfer because $\Delta E_m = 0$. The smallest value of $(T_{DA})^2$ weighted by the Franck-Condon factor for heme $b_p \to b_p$ electron transfer, 2.2×10^{-16}, is approximately an order of magnitude larger than that of heme $b_p \to b_n$ electron transfer (Table 3). Thus, it would seem that inter-monomer $b_p \to b_p$ electron transfer (Fig. 3) must be considered feasible on structural grounds, and electron sharing between hemes b_p must be considered in mechanistic descriptions of function of the cytochrome bc_1 and, probably, b_6f complexes.

ELECTRON TRANSFER FROM QUINOL TO HIGH AND LOW POTENTIAL CHAINS

The one-electron reduction of $QH_2 \to QH_2^+$ has an $E_m = +900$ mV (Rich, 1984). This potential is too positive for electron transfer to any of the b_6f or bc_1 redox centers. Upon deprotonation and subsequent formation of the semiquinone ($QH^- \to QH^{\bullet} + e^-$), the E_m value decreases to $+200$ mV. This initial deprotonation is necessary to initiate the events of the Q-cycle, and has been found to be its rate-limiting step (Brandt and Okun, 1997). The identity of the signal that triggers quinol deprotonation is not known, but it must be an "oxidation-induced deprotonation." From the classical studies on "oxidation-induced reduction" (Wikstrom and Berden, 1972; Trumpower, 1981), cyt c_1 or cyt f must be initially oxidized to trigger reduction of cyt b. The signal to the Q_{p1} niche that triggers the quinol pK change is then presumably carried by the mobile ISP [see reviews (Berry *et al.*; Iwata *et al.*) of ISP mobility in this volume]. In cyt bc_1 co-crystallized with the quinone analog stigmatellin, which binds at the Q_{p1} site, one of the ligands of the [2Fe–2S] cluster, His161, is within hydrogen-bonding distance (~ 3.0 A) of the stigmatellin. At this position, the ISP could influence the environment of the Q_{p1} niche, leading to the first deprotonation, and electron transfer from $QH^{\bullet}$ to the high-potential chain occurs efficiently. The transfer of the second electron to heme b_p may be

controlled by: (i) an increase in the ISP midpoint potential upon binding of the quinol to one of the Rieske His ligands (Link, 1997). This effect would probably be more important in b_6f than in bc_1, because the the E_m of cyt c_1 is already less than that of ISP in mitochondrial and bacterial bc_1. (ii) Transfer of the second electron to heme b_p and the low potential chain, and imposition of the bifurcated electron transfer would follow movement of the neutral semiquinone to the Q_{p2} (myxothiazol or MOA-stilbene) site, where it is more distant from the ISP and is closer to heme b_p. Alternatively, the semiquinone function could be transferred through two bound quinones (Ding *et al.*, 1992; Brandt, 1998). It is of interest that electron transfer from the Q_{p1} site to heme b_p does not seem *a priori* to be excluded. The attenuation factor, $(TDA)^2 = 2–3 \times 10^{-14}$ for transfer from the O12 of stigmatellin through three through-space and five covalent bonds. This factor is in the range of the factors calculated for the transfers between hemes b. However, the actual value of the Em of the semiquinone is not known and this will affect the contribution of the Franck-Condon term to the rate of electron transfer.

ET from the semiquinol at the myxothiazol site to heme b_p can occur efficiently, using two through-space jumps (Ed Berry, personal communication): (a) 3.5 A from myxothiazol to Tyr274 (part of the conserved PEW·Y sequence in both b_6f and bc_1 complexes) and (b) 3.8 A from Tyr274 to heme b_p. These through-space jumps would give an activationless attenuation factor, $(TDA)^2 = 7 \times 10^{-11}$, 300–400 times larger than calculated above for transfer from the Q_{p1} site. The presence of two Q_p, binding sites would ensure bifurcation of electron transfer from the quinol to the high and low-potential chains.

The two quinone species that were inferred to occupy sites proximal and distal to the ISP iron-sulfur cluster have the property of strong and weak binding, Q_{pw} (weak) and Q_{ps} (strong) (Ding *et al.*, 1992). Alternatively, the different positions occupied by stigmatellin and myxothiazol could be the positions of the quinone before and after electron transfer to the Rieske protein. In this case, the neutral deprotonated QH· has to move from the "Rieske" position to the "b" position after electron transfer to the ISP. The second possibility seems more likely because the protein might undergo large conformational changes to fit two quinones at the Q_p sites (Crofts and Berry, 1998). The absence of tightly bound quinone at the Q_p sites in the native bc_1 crystals and the presence of ubiquinone at the Q_n site in some bc_1 crystals grown with ubiquinone

(pdb1BCC.ent) argue against the existence of Q_{ps} quinone.

p-SIDE PROTON TRANSFER

The release of two protons ($H^+/e^- = 2$) to the *p*-side lumenal aqueous phase is associated with (i) deprotonation of the neutral quinol, $QH_2 \rightarrow QH^- + H^+$, that initiates the *p*-side election and proton transfer and, (ii) subsequently, deprotonation of the anionic semiquinol ($QH^· \rightarrow Q^{·-} + H^+$) that could occur at sites close to Q_{p1} (stigmatellin) and Q_{p2} (myxothiazol/MOA-stilbene) [Fig. 4].

Deprotonation of the Neutral Quinol, $QH_2 \rightarrow QH^- + H^+$

The following data bear on the properties and pathway of release of the first proton. The dependence of the *p*-side reactions in the mitochondrial bc_1 complex on linked proton transfer is shown by: (a) an isotope effect, $k_{H2O}/k_{D2O} \sim 1.4–1.7$ at pH 8.0 for the cyt c reductase activity of isolated bc_1 complex; (b) the pH dependence of the activation energy for electron transfer from decyl-ubiquinol, which varies by -5.7 kJ/pH unit, and is consistent with dissociation of a single proton. This implies that the initial quinol depro-
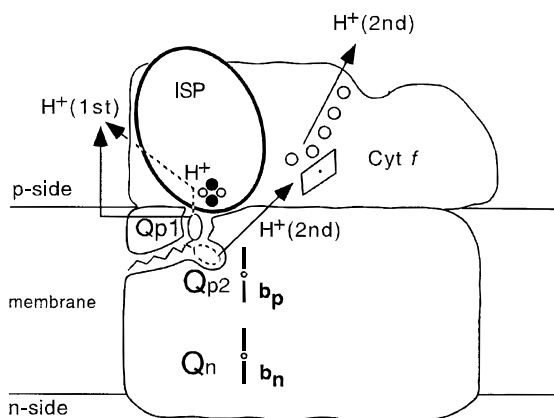
Fig. 4. Model for *p*-side proton transfer and deposition. Release of two protons ($H^+/e = 2$) is associated with deprotonation of the neutral quinol and, subsequently, the neutral semiquinone at the stigmatellin (Q_{p1}) and myxothiazol/MOA-stilbene (Q_{p2}) sites, with subsequent transfer to the *p*-side bulk aqueous phase from Q_{p1} through cyt b and/or ISP, and from Q_{p2} through cyt b and cyt f and its internal water chain.

tonation is the rate-limiting step in the overall reaction (Brandt and Okun, 1997).

The kinetics of cyt f reduction decrease monotonically from pH 5.5-6.5, while remaining almost constant between pH 6.5 and 8.0 (Nishio and Whitmarsh, 1993). This behavior correlates with a $pK_{OX} = 6.5$ for the b6f Rieske fragment (Zhang $et\ al.$, 1996) if electron transfer from the quinol to ISP requires a deprotonated ISP. An isotope effect, $k_{H2O}/k_{D2O} = 1.4$-2.0 at pH or pD 7.5 was also observed for the light-induced slow electrochromic bandshift associated with uncompensated charge transfer through the b_6f complex (Farineau $et\ al.$, 1980; Soriano and Cramer, 1999), and for reduction of cytochromes f and b_6 in the high and low potential chains (Soriano and Cramer, 1999). This suggests that the same deprotonation step, presumably deprotonation of plastoquinol, limits the rates of both electron transfer reactions. The pathway of proton transfer from the quinol to the p-side aqueous phase may traverse residues in the cyt b polypeptide and/or the ISP. The $N\delta1$ nitrogen of the His161 ligand of the bovine ISP (His 128 in the b_6f ISP) has been suggested as a proton acceptor (Link $et\ al.$, 1996). A major problem with this suggestion, particularly in the acidic environment of the chloroplast lumen, is the high pK (9–14) of the imidazolate nitrogen at the $N\delta1$ position. This could be decreased by coordination of the $N\varepsilon$ to the cluster Fe. However, in the ambient pH ~ 5 of the chloroplast lumen, it seems hard to avoid permanent protonation of the imidazole $N\delta1$ of the cluster ligands, His128 and 109.

Deprotonation Pathway of the Neutral Semiqunone, $QH^{\cdot} \rightarrow Q^{\cdot-} + H^+$

Assuming that the neutral semiquinone is deprotonated at the site, Q_{p2}, and that the exit pathway from the membrane utilizes the internal water chain of cyt f, one is led to search for a possible proton transfer pathway from region of Q_{p2} to cyt c_1 in the structure of bc_1. The following are suggestions for two such pathways (numbering from chicken bc_1 complex; E. Berry, pers. comm.) that could provide a H^+ transfer path from Q_{p2} to cyt f: (a) H^+ transfer 5.3 Å from the MOA-stilbene O3 to $O\varepsilon3$ of Glu272 of the conserved PEWY sequence (residues $_{77}$PEWY$_{80}$ in suIV); from E272 over 8 Å to Lys270, from Lys270 5.3 Å to Asp 253, and 5.3 Å from Asp253 to the $N\varepsilon2$ of His121 of cyt c_1. (b) The second pathway from the myxothiazol Q_{p2} site would involve H^+ transfer over 3.5Å to the

$-$OH of the Tyr274 of PEWY, 4.4 Å from Tyr274 to the $O\varepsilon2$ of Glu272 of PEWY, 8.6 Å from Glu272 to Lys 270, and 6.2 Å from Lys270 to the $N\varepsilon2$ of His 121 of cyt c_1. These pathways described as that of proton "2" in Fig. 4 are surely incomplete even if some H^+-carrier residues have been identified. The large inter-residue distances would require conformational changes and/or bound H_2O molecules (Luecke $et\ al.$, 1998) to bridge the gaps.

The PEWY sequence, in the p-side peripheral "ef" helix of suIV and cyt b, has long been suspected to be important in p-side charge transfer from its high degree of sequence identity (Widger $et\ al.$, 1984; Degli Esposti $et\ al.$, 1993). A test of its critical function was provided by site-directed mutants, E78K, E78N, E78Q and E78L, generated in the b_6f complex of $Chlamydo$-$monas\ reinhardtii$ (Zito $et\ al.$, 1998). These mutants show a decrease, relative to the wild type, in the rate of: (i) onset of the slow electrochromic bandshift ($t_{1/2}$ increased from 7 to 16 ms), (ii) cyt b_6 reduction ($t_{1/2}$ increased from 2.5 to 8.5 ms in the presence of NQNO) and oxidation, and (iii) cyt f reduction ($t_{1/2}$ increased from 2.2 ms to 10.2 ms for the neutral mutants and 6 ms for Lys mutants) (Zito $et\ al.$, 1998). Substitution with aspartate (E78D) did not cause any observable change in the rates of the electron transfer reactions, and the E78L mutant showed the most drastic effect. The decrease in rate constants of the slow electrochromic phase and electron transfer in both the high and low potential chains was explained as a consequence of a decrease in the rate of quinol oxidation. Slower quinol oxidation was also observed in PEWY mutants of the bc_1 complex of $Rb.\ sphaeroides$, the V_{max} for E295D, E295G and E295Q decreasing 2-, 9- and 50-fold relative to wild type rates (Crofts $et\ al.$, 1995).

DCCD Experiments

Chemical modification of isolated b_6f complex with DCCD, a known modifier of carboxyl groups in hydrophobic environments, resulted in $\sim 60\%$ inhibition of proton pumping but only $\sim 20\%$ inhibition of electron transfer to cytochrome (Wang and Beattie, 1991). A similar behavior was observed in DCCD-treated bc_1 complexes (Wang $et\ al.$, 1998). It is difficult in such experiments to modify only one or a few residues, but preferential labeling could be determined of Asp155 and/or Glu166 in the "cd" loop by ^{14}C-labelling of isolated cyt b_6 (Wang and Beattie, 1992).

Subunit IV was not labeled perhaps because the environment of E78 was too hydrophilic. In experiments on the effects of DCCD labeling of algal cells (Joliot and Joliot, 1998), the rates of reduction of cyt *b* and cyt *f* were inhibited and a lag appeared in the slow electrochromic bandshift. These data were interpreted in terms of the blocking of a proton acceptor for the rate-limiting quinol deprotonation at the Q_{pl} site, and also of residues in the *n*-side H^+ uptake network.

ACKNOWLEDGMENT

REFERENCES

Alberts, B., Bray, D., Lewis, J., Raff, M., Roberts, K., and Watson, J. D. (1994). *Molecular Biology of the Cell*, Garland Publishing, New York.

Beratan, D. N., and Onuchic, J. N. (1996). In *Protein Electron Transfer* (Bendall, D. S., ed.), BIOS Scientific Publishers, Oxford, pp. 23–42.

Berry, E. A., Huang, L.-S., Chi, Y., Zhang, Z., Malkin, R., and Fernandez-Velasco, J. G. (1997). *Biophys. J.* **72**, A125.

Brandt, U. (1998). *Biochim. Biophys. Acta* **1365**, 261–268.

Brandt, U., and Okun, J. G. (1997). *Biochemistry* **36**, 11234–11240.

Buschlen, S. (1993). ENTREZ database acc. no. 421760

Buschlen, S., Choquet, Y., Kuras, R., and Wollman, F. A. (1991). *FEBS Lett.* **284**, 257–262.

Carrell, C. J., Zhang, H., Cramer, W. A., and Smith, J. L. (1997). *Structure* **5**, 1613–1625.

Carrell, C. J., Schlarb, B. G., Bendall, D. S., Howe, C. J., Cramer, W. A., and Smith, J. L. (1999). *Biochemistry*, **38**, 9590–9599.

Chain, R., and Malkin, R. (1991). *Photosynth. Res.* **28**, 59–68.

Cramer, W. A., Black, M. T., Widger, W. R., and Girvin, M. E. (1987). In *The Light Reactions* (Barber, J., ed.), Elsevier, Amsterdam, pp. 446–493.

Crofts, A. R., and Berry, E. A. (1998). *Curr. Opin. Struct. Biol.* **8**, 501–509.

Crofts, A. R., and Wang, Z. (1989). *Photosynth. Res.* **22**, 69–87.

Crofts, A. R., Barquera, B., Bechmann, G., Guergova, M., Salcedo-Hernandez, R., Hacker, B., Hong, S., and Gennis, R. B. (1995). In *Photosynthesis: From Light to Biosphere* (Mathis, P., ed.), Kluwer Academic Publishers, Dordrecht, pp. 493–500.

de Vitry, C. (1994). *J. Biol. Chem.* **269**, 7603.

de Vitry, C., Breyton, C., Pierre, Y., and Popot, J.-L. (1996). *J. Biol. Chem.* **271**, 10667–10671.

Degli Esposti, M., De Vries, S., Crimi, M., Ghelli, A., Patarnello, T., and Meyer, A. (1993). *Biochim. Biophys. Acta* **1143**, 243–271.

Ding, H., Robertson, D. E., Daldal, F., and Dutton, P. L. (1992). *Biochemistry* **31**, 3144–3158.

Farid, R. S., Moser, C. S., and Dutton, P. L. (1993). *Curr. Opin. Struct. Biol.* **3**, 225–233.

Farineau, J., Garab, G., Horvath, G., and Faludi-Daniel, A. (1980). *FEBS Lett.* **118**, 119–122.

Fong, S. E., and Surzycki, S. J. (1992). *Curr. Genet.* **21**, 527–530.

Furbacher, P. N., Tae, G.-S., and Cramer, W. A. (1996). In *Origin and Evolution of Biological Energy Conversion* (Baltscheffsky, H., ed.), pp. 221–253, VCH Publishers, New York.

Gray, H. B., and Winkler, J. R. (1996). *Annu. Rev. Biochem.* **65**, 537–562.

Haehnel, W. (1975). In *Proceedings of the 3rd International Congress on Photosynthesis* (Avron, M., ed), Elsevier, Amsterdam, pp. 557–558.

Hauska, G., Hurt, E., Gabellini, N., and Lockau, W. (1983). *Biochim. Biophys. Acta* **726**, 97–133.

Heimann, S., Ponamarev, M. V., Piskorowski, R. and Cramer, W. A. in preparation (1999).

Huang, D., Everly, R. M., Cheng, R. H., Heymann, J. B., Schagger, H., Sled, V., Ohnishi, T., Baker, T. S., and Cramer, W. A. (1994). *Biochemistry* **33**, 4401–4409.

Huang, D., Zhang, H., Soriano, G. M., Dahms, T. E. S., Krahn, J. M., Smith, J. L., and Cramer, W. A. (1999). In *Photosynthesis: Mechanisms and Effects* (Garab, G., ed.), Kluwer Academic Publishers, Dordrecht, pp. 1577–1580.

Iwata, S., Lee, J. W., Okada, K., Lee, J. K., Iwata, M., Rasmussen, B., Link, T. A., Ramaswamy, S., and Jap, B. K. (1998). *Science* **281**, 64–71.

Joliot, P., and Joliot, A. (1998). *Biochemistry* **37**, 10404–10410.

Ketchner, S. L., and Malkin, R. (1996). *Biochim. Biophys. Acta* **1273**, 195–197.

Kim, H., Xia, D., Yu, C. A., Xia, J. Z., Kachurin, A. M., Zhang, L., Yu, L., and Deisenhofer, J. (1998). *Proc. Natl. Acad. Sci. U.S.* **95**, 8026–8033.

Kraulis, P. J. (1991). *J. Appl. Crystallogr.* **24**, 946–950.

Kuras, R., Guergova-Kuras, M., and Crofts, A. R. (1998). *Biochemistry* **37**, 16280–16288.

Link, T. A. (1997). *FEBS Lett.* **412**, 257–64.

Link, T. A., Saynovits, M., Assmann, C., Iwata, S., Ohnishi, T., and von Jagow, G. (1996). *Europ. J. Biochem.* **237**, 71–75.

Luecke, H., Richter, H. T., and Lanyi, J. K. (1998). *Science* **280**, 1934–1937.

Marcus, R., and Sutin, N. (1985). *Biochim. Biophys. Acta* **811**, 265–322.

Martinez, S. E., Huang, D., Szczepaniak, A., Cramer, W. A., and Smith, J. L. (1994). *Structure* **2**, 95–105.

Martinez, S., Huang, D., Ponomarev, M., Cramer, W. A., and Smith, J. L. (1996). *Protein Sci.* **5**, 1081–1092.

Matsumoto, T., Matsuo, M., and Matsuda, Y. (1991). *Plant Cell Physiol.* **32**, 863–872.

Merritt, E. A., and Murphy, M. E. P. (1994). *Acta Crystallogr.* **D50**, 869–873.

Moser, C. C., Page, C. C., Farid, R., and Dutton, P. L. (1995). *J. Bioenerg. Biomembr.* **27**, 263–274.

Mosser, G., Breyton, C., Olofsson, A., Popot, J. L., and Rigaud, J. L. (1997). *J. Biol. Chem.* **272**, 20263–20268.

Nishio, J. N., and Whitmarsh, J. (1993). *Plant Physiol.* **101**, 89–96.

Pierre, Y., Breyton, C., Krumer, D., and Popot, J. L. (1995). *J. Bio. Chem.* **270**, 29342–29349.

Ponamarev, M. V. (1999). Ph.D. thesis. *Structure-Function Relationships in Cytochrome f of Oxygenic Photosynthesis*. Purdue University, 134 pp.

Ponamarev, M. V., and Cramer, W. A. (1998). *Biochemistry* **37**, 17199–17208.

Rich, P. (1984). *Biochim. Biophys. Acta* **768**, 53–79.

Saraste, M. (1984). *FEBS Lett.* **166**, 367–372.

Selak, M. A., and Whitmarsh, J. (1982). *FEBS Lett.* **150**, 286–292.

Soriano, G. M., and Cramer, W. A. (1999). Unpublished data.

Soriano, G. M., Ponamarev, M. V., Piskorowski, R. A., and Crumer, W. A. (1998) *Biochemistry* **37**, 15120–15128.

Soriano, G. M., Ponamarev, M. V., Tae, G.-S., and Cramer, W. A. (1996). *Biochemistry* **35**, 14590–14598.

Takahashi, Y., Rahire, M., Breyton, C., Popot, J.-L., Joliot, P., and Rochaix, J.-D. (1996). *EMBO J.* **15**, 3498–3506.

Trumpower, B. L. (1981). *Biochim. Biophys. Acta* **639**, 129–155.

Wang, Y., and Beattie, D. S. (1991). *Arch. Biochem. Biophys.* **291**, 363–370.

Wang, Y., and Beattie, D. S. (1992). *Biochemistry* **31**, 8455–8459.

Wang, Y. D., Obungu, V., and Beattie, D. S. (1998). *Arch. Biochem. Biophys.* **352**, 193–198.

Whitmarsh, J., Bowyer, J. R., and Crofts, A. R. (1982). *Biochim. Biophys. Acta* **682**, 404–412.

Widger, W. R., Cramer, W. A., Herrmann, R. G., and Trebst, A. (1984). *Proc. Natl. Acad. Sci. U.S.* **81**, 674–678.

Wikstrom, M. K. F., and Berden, J. A. (1972). *Biochim. Biophys. Acta* **283**, 403–420.

Xia, D., Yu, C.-A., Kim, H., Xia, J.-Z., Kachurin, A. M., Yu, L., and Deisenhofer, J. (1997). *Science* **277**, 60–66.

Yun, C.-H., Wang, Z., Crofts, A. R., and Gennis, R. B. (1992). *J. Biol. Chem.* **267**, 5901–5909.

Zhang, H., Carrell, C. J., Huang, D., Sled, V., Ohnishi, T., Smith, J. L., and Cramer, W. A. (1996). *J. Biol. Chem.* **271**, 31360–31366.

Zhang, Z., Huang, L., Shulmeister, V. M., Chi, Y. I., Kim, K. K., Hung, L. W., Crofts, A. R., Berry, E. A., and Kim, S. H. (1998). *Nature* **392**, 677–684.

Zhang, H., Huang, D., and Cramer, W. A. (1999a). *J. Biol. Chem.* **274**, 1581–1587.

Zhang, H., Rakich, P., Nolte, D., and Cramer, W. A. (1999b). Unpublished data.

Zhou, J., Fernandez-Velasco, J., and Malkin, R. (1996). *J. Biol. Chem.* **271**, 6225–6232.

Zito, F., Finazzi, G., Joliot, P., and Wollman, F. A. (1998). *Biochemistry* **37**, 10395–10403.